

Structure mapping at Trap Spring Oilfield, Nevada, using controlled-source magnetotellurics *

Larry J. Hughes † & Norman R. Carlson †

The seismic reflection method has been a highly successful tool in oil and gas exploration for half a century, and it presently accounts for about 98% of all geophysical expenditures world-wide. However, the relatively high cost of seismic exploration and its limitations in certain geologic environments are continuing problems. Some help has been provided by the magnetotelluric (MT) sounding technique, but the cost of MT is also quite high due to the low natural signal strengths being measured.

The controlled-source audio-frequency magnetotellurics (CSAMT) technique is a shallower-penetrating variation of MT which uses an artificial signal source. This permits faster and more economical data acquisition. CSAMT has a penetration of about 2 km in typical petroliferous environments. CSAMT does not replace seismic but functions in three specific roles: (1) as a reconnaissance tool to help focus seismic coverage, or to help avoid 'no-record' zones; (2) to assist in static corrections and in interactive seismic interpretation; (3) as a primary tool in certain environments (volcanics, complex thrust areas) where seismic data acquisition is limited.

An example of the application of CSAMT to structure mapping comes from data taken over Trap Spring Field, located in the frontier Great Basin of the western United States. The field produces oil from fractured volcanics at the edge of a major graben fault. The CSAMT data delineate the major subsurface faulting and stratigraphic relationships in the area. The resolution of the CSAMT survey is significantly better than previously obtained induced polarization (IP) data. Detailed comparisons with electric log, drill hole, and air-photo data show an excellent correlation between the CSAMT features and known geology. The work suggests that CSAMT could be used in this area for reconnaissance mapping to develop seismic prospects, at approximately one sixth the cost of seismic.

Introduction

Since its development in the 1930s, the seismic reflection technique has proved to be an invaluable geophysical tool in exploration for oil and natural gas. Its inherent resolving power has made it particularly effective in mapping subsurface structure and stratigraphy. As a result, seismic now represents about 98% of total world wide expenditure on geophysics (Montgomery 1985). However, the steady trend towards increasingly difficult exploration targets has not only made seismic more expensive, but also has led explorationists into some frontiers where seismic is less effective. In recent years a renewed emphasis has been placed upon multi-disciplinary exploration in order to offset these problems.

An important group of supplementary geophysical techniques has been electrical and electromagnetic methods. The most familiar electrical technique in petroleum exploration has been magnetotellurics (MT) but other methods such as controlled source audio-frequency MT (CSAMT), transient electromagnetics (TEM), and induced polarization (IP) have been frequently used. In general these techniques have had five distinct applications, in decreasing order of success: (1) structure mapping; (2) mapping possible near-surface electrochemical alteration due to microseepage from deeper traps; (3) detecting and monitoring brine and hydrocarbon contaminants from injection wells and refining facilities; (4) monitoring secondary recovery processes; (5) direct detection of very shallow oil-bearing strata. At this time the structure-mapping application is probably the most effective and best-documented use of electrical methods for petroleum exploration.

Since seismic is superior to electrical in terms of resolution, electrical methods are best viewed as a complementary, not a competitive, geophysical approach. In this context, electrical techniques have three primary contributions to a seismic exploration programme: (1) mapping frontier areas on a reconnaissance basis in order to isolate specific prospects for more expensive seismic detailing; (2) complementing seismic interpretation with additional structural or lithologic information; (3) replacing

* Paper presented at the 48th Meeting of the European Association of Exploration Geophysicists, Ostend, June, 1986.

† Zonge Engineering & Research Organization, Inc., 3322 East Fort Lowell Road, Tucson, AZ 85716 USA.

seismic in very difficult environments, such as in basins where productive sediments are overlain by thick basalts.

This paper illustrates the use of the CSAMT technique for mapping petroleum-related structure on a reconnaissance basis, and points out how the technique might be used in a multi-disciplinary exploration programme.

The CSAMT technique

Controlled-source audio-frequency magnetotellurics (CSAMT) is a high-resolution electromagnetic sounding technique which utilizes an artificial grounded dipole as a signal source. It was first proposed by Goldstein & Strangway (1975) as a method of overcoming the weak ambient signal levels associated with the natural-source magnetotelluric (MT) technique. The result has been a more economic version of MT for targets within the top few kilometres of the surface.

Since its first commercial use in the late 1970s, CSAMT has been used in a variety of applications. These include the mapping of small-scale and large-scale structural features for petroleum exploration (Hughes 1984; Hughes *et al.* 1984), mapping possible electrochemical alteration in the sediments above oilfields (Ostrander *et al.* 1983; Hughes *et al.* 1984),

monitoring secondary oil recovery operations (Bartel & Wayland 1981; Wayland *et al.* 1984; Wayland & Leighton 1985), mapping burn fronts in underground coal gasification projects (Bartel 1982), coal exploration (Bartel & Dobecki 1982), exploration for geothermal resources (Sandberg & Hohmann 1982; Bartel & Jacobson 1987; Yamashita *et al.* 1985), mapping groundwater contamination (Fryberger & Tinlin 1984; Zonge *et al.* 1985), and mapping conductive mineralization (Zonge *et al.* 1980; Lakanen 1986; Hjelt *et al.* 1987). The authors also have applied CSAMT for mapping structure related to occurrences of sulphur, uranium, precious metals, and coal, for monitoring reservoir fluids in geothermal fields, for mapping brine contamination of drinking water supplies from leaks in injection wells and pipelines, and for mapping spills of refined hydrocarbons.

The CSAMT signal source consists of one or two grounded dipoles (Fig. 1). Signals at levels of tens of amperes and across a frequency band of 0.1 to 10000 Hz are used in most CSAMT surveys. The measurements consist of key components of the electric and magnetic fields at points some 5 to 15 kilometres from the sources. In complex geology, full-tensor measurements (10 field components, two orthogonal sources) are required, as

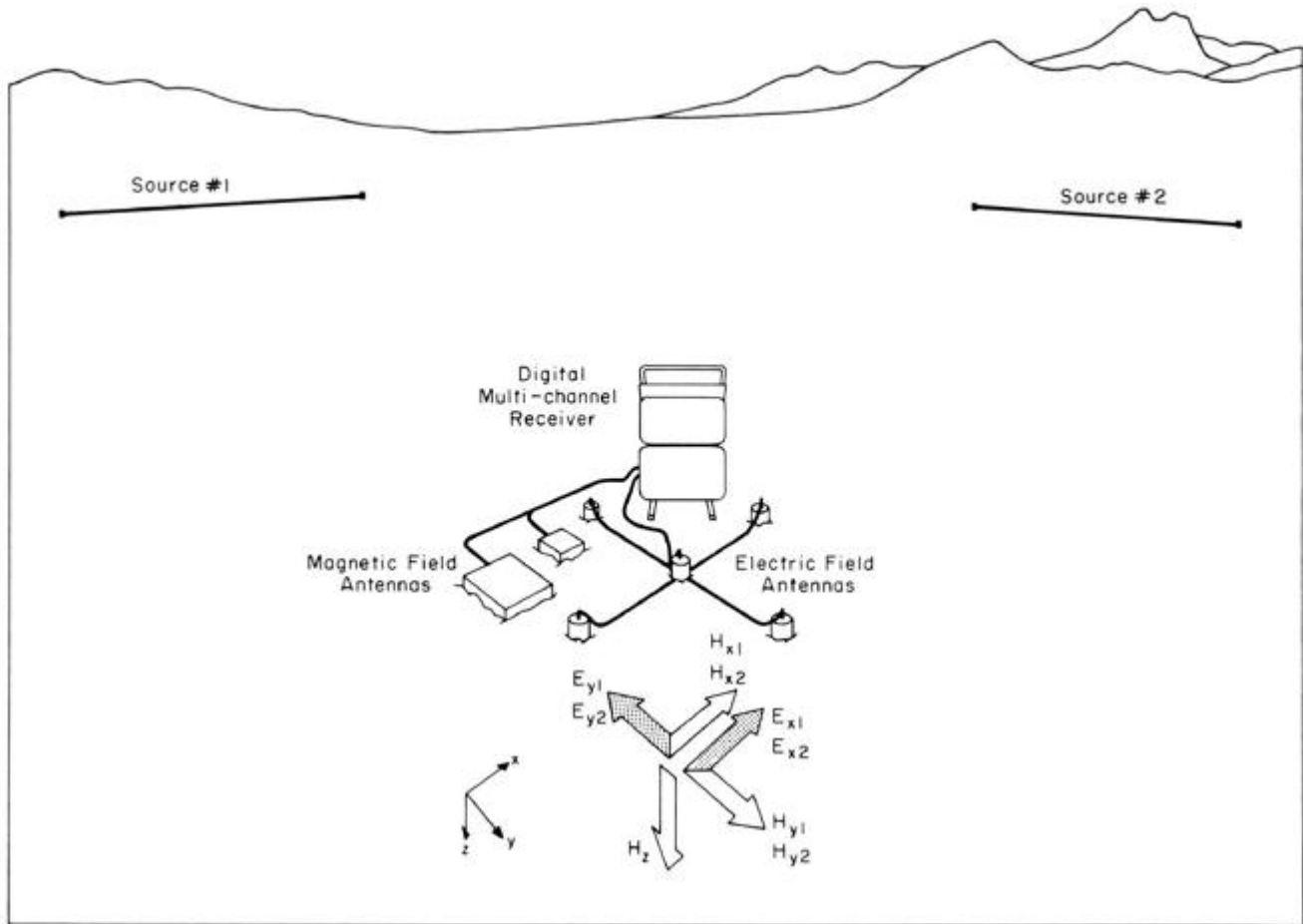


Fig. 1. Field set-up for tensor CSAMT. Areas with relatively simple geology may permit acquisition of scalar data (E_{x1} and H_{y1} from source No. 1 only), as in the present data set.

illustrated in Fig. 1. The use of two distinct sources best simulates the multiple-polarity source used in MT work. Tensor CSAMT data are rotated to their principal directions to obtain resistivity / phase data parallel and perpendicular to strike, much as is done in MT. Less complex geology may call for vector (four components, two sources) or scalar (two components, one source) measurements. In very simple geology, one can utilize a variation on CSAMT known as controlled-source audio-frequency electrotellurics (CSAET). In CSAET, only a single electric field component is measured at each station, and occasional magnetic field measurements are made to generate apparent resistivity data.

Penetration and resolution

The penetration of CSAMT on conductive environments is less than a skin depth, where skin depth δ in metres is defined as

$$d = 503 \sqrt{\frac{2\rho r}{\omega}} \quad d = \sqrt{\frac{2r}{\omega\mu}}$$

where ρ is the ground resistivity in ohm-metres, ω is the angular frequency in radians per second and μ is the magnetic permeability. Hence, in typical petroliferous environments (10 to 100 ohm-metres resistivity), a maximum penetration of 3.5 to 11 km is possible for low frequencies on the order of 0.1 Hz. In general, however, we have found that the practical limit is about 2 km, given considerations of signal strength and the need to keep all measurements as far from the source as possible. Hence the technique does not replace conventional magnetotellurics, but serves as a near-surface supplement to it.

Lateral resolution of CSAMT data is roughly equivalent to the electric field dipole length, which typically is 30 to 300 m. Vertical resolution of conductive features is roughly 20% of the depth of burial. This is crude by seismic standards, but is usually sufficient for the purposes to which CSAMT is applied.

In general, tensor CSAMT costs about one fourth the cost of magnetotellurics. This is partly due to the different frequencies measured (CSAMT 0.125 to 10000 Hz; MT 0.001 to 200 Hz), and partly due to signal improvement with the CSAMT source.

Source effects

Unlike the MT situation, where the source is thought of as infinitely distant and non-polarized, the CSAMT source is finite in distance and is distinctly polarized in terms of orientation. This leads to two important considerations in interpretation: non-plane-wave or geometric effects, and source overprint effects.

Non-plane-wave effects arise due to the finite separation, r , between the source and the sounding point. The measurement zone far from the source ($r > 4\delta$) is known as the 'far-field zone'; closer to the source ($0.56 < r < 4\delta$) is the 'transition zone', and very close to the source ($r < 0.5\delta$) is the 'near-field zone'.

In the far-field zone, the impinging electromagnetic wave can be thought of as a plane-wave propagating vertically into the Earth. This simulates the MT case and is thus the desired configuration for CSAMT work. Our modelling (Zonge & Hughes 1988) has shown that calculated resistivities are within 5% of the actual ground resistivities when $r > 4\delta$ for the electric field measurements parallel to the source. Under this condition the measured resistivities are independent of source- sounding separation or geometry. The far-field apparent resistivity ρ_a , often referred to as the 'Cagniard resistivity', can be calculated from the ratio of orthogonal electric and magnetic field components according to

$$r_a = 0.2T \left(\frac{E_x}{H_y} \right)^2$$

in which E_x is the electric field strength in some horizontal direction in nV km⁻¹, H_y the magnetic field strength in the perpendicular horizontal direction in gammas, and T is the period in seconds, to give the resistivity in ohm-metres. A second parameter, phase difference, is also measured:

$$j = j_E - j_H$$

in which ϕ_E is the phase angle of the electric field referenced to the source signal, and ϕ_H is the corresponding phase angle of the magnetic field. A phase difference of $\pi/4$ or 785.4 milliradians corresponds to an homogeneous earth response; larger values suggest high-over-low resistivity layering; smaller values suggest low-over-high layering.

In the near-field zone close to the source, the impinging wave does not behave like a plane wave, and the apparent resistivity is much more complex than in the simple Cagniard relationship. In addition, the magnetic field becomes 'saturated', or independent of frequency and resistivity (Zonge & Hughes 1988). This has the important implication that the data are no longer 'sounding' according to the skin-depth relationship, but that depth penetration is a direct function of geometry between the source and the measurement point. Hence, near-field data behave more like a dipole-dipole induced polarization survey than an electromagnetic sounding survey. The near-field zone is avoided whenever possible. The distorting effects of the near-field zone on the Cagniard resistivity calculation are shown in Fig. 2.

In the transition zone between the near-field and far-field zones, resistivities are partly a function of geometry, and soundings are controlled by both frequency and geometry. The transition zone often can be identified in Cagniard resistivity data as a dip or 'notch' and then a steep rise in resistivity as one progresses to lower frequencies. The notch is always shallow in relatively homogeneous environments, but becomes more pronounced in geology where low-over-high resistivity layering is found. When such layering occurs at the depth corresponding to the effective penetration at the notch frequency, the notch shape becomes very sensitive to geologic changes. In such a case the notch

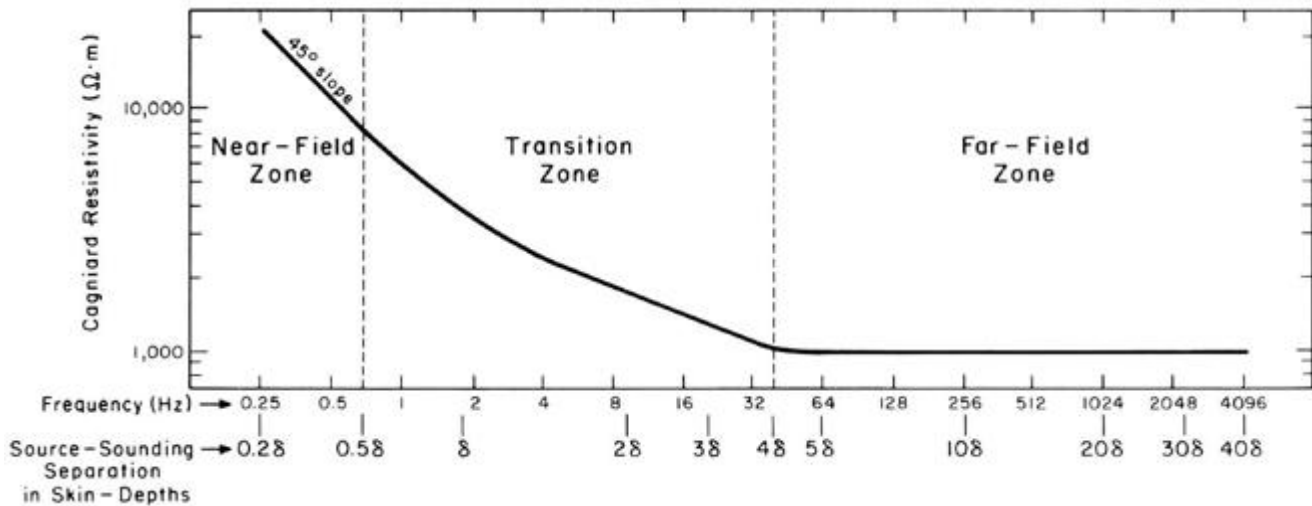


Fig. 2. CSAMT Cagniard resistivity in a 1000 ohm-m homogeneous earth, illustrating near-field effects. At a source-sounding separation, r , exceeding four skin-depths, the transition zone distorts the true resistivity; at $r < 0.5$ skin-depths, the near-field zone causes saturation of the signal and prevents proper data acquisition.

is said to be 'tuned' by the geology. The data presented in this paper illustrate how this can actually enhance interpretation.

In addition to non-plane-wave effects, the source has an effect on the measurements known as 'source over print' (Zonge *et al.* 1980; Zonge & Hughes 1988). Source overprint occurs when the geology beneath the source differs from the geology beneath the sounding. The result is an overprint of the geologic effects beneath the source on to the data collected at the sounding point. The effect is usually small in the far-field data but can be pronounced in the transition and near-field zones. In particular, overprint often has the result of shifting the incursion of near-field effects to higher frequencies than normally expected. The data in this paper provide a good illustration of this phenomenon.

Static effect

Possibly the most significant interpretational problem in MT and CSAMT is the so-called static effect (Larsen 1981; Warner *et al.* 1983; Sternberg *et al.* 1984). As described by Zonge & Hughes (1988), this effect can occur due to the presence of a near-surface, finite, electrically inhomogeneous body. The problem can be visualized as the result of a static charge distribution which accumulates at the surface of the body. When the size of the body is smaller than the wavelength of the investigating signal, the body is no longer resolved directly. Instead, the surface charge produces a frequency-independent 'static shift' of the apparent resistivity data. The net result is that resistivity data, plotted versus frequency on logarithmic scales, will be shifted up and down, depending on the resistivity of the body and location of the sounding point. This is a serious problem, as it can throw off estimated depths and can result in an erroneous interpretation of subsurface effects.

Some investigators (Andrieux & Wightman 1984; Sternberg *et al.* 1985) have experimented with correcting static effects in MT data with additional transient electromagnetics (TEM) measurements. An alternative approach, developed by Zonge (Zonge & Hughes 1988), involves an integration of phase difference data (which are unaffected by static offset) and shifting the results by a factor computed by average resistivities for specified stations and frequencies. An example is provided in the case history.

Case history: Trap Spring Field

Geologic Setting

Trap Spring Field is located in the Railroad Valley sub-basin of the Great Basin, which lies in the western interior of the United States (Fig. 3). Railroad Valley is a semi-arid, single-valley basin surrounded to the east and west by the Pancake and Grant mountain ranges. The 160-km long, 3000-km valley was formed by the late Tertiary basin-and-range graben faulting which is typical of the western two-thirds of the Great Basin.

All presently known Railroad Valley oilfields lie on the downthrown sides of the graben faults which control the edges of the valley (Fig. 4). Trap Spring Field occurs along the graben fault which bounds the western side of the valley (Fig. 5). As described in detail by numerous authors (Duey 1979; Foster 1979; French & Freeman 1979; Dolly 1979), the trap occurs in the Pritchards Station Formation, a multiple-flow, Oligocene ignimbrite unit. The reservoir rock was deposited from local volcanic vents along relatively flat topography, and was later faulted and fractured by basin-and-range tectonism. The oil is found in joints and fractures formed by faulting and by the rapid cooling of the volcanics



Fig. 3. General location of Trap Spring Field.

following deposition. The reservoir is a combination structural-and-stratigraphic type. It is limited laterally by sealed faults, the oil-water contact, and loss of reservoir permeability. The top seal is provided by an ash zone which has been heavily altered to clay; the bottom seal is caused by a loss of reservoir porosity due to vitrification at the base of the ignimbrite flow.

Overlying the volcanics is a thick section of heterogeneous alluvial overburden (Fig. 5c). The lower portion of the overburden consists of sands, silts and shale material, and lithic fragments of the Tertiary Horse Camp Formation; the upper portion involves Quaternary and more recent clay, silty sandstones and evaporite deposits. Within the sediments are considerable changes in grain size and groundwater salinity, as well as interbedded volcanic lenses, gravity slides, and lithic inclusions.

Oil of 21° to 28° API gravity and no gas is produced from 26 wells. As of February 1986, some 6.4 million barrels of oil had been produced, and the field is still under active development on its northern flank.

Exploration problems

The 400000-km² Great Basin is a highly underdeveloped frontier area which had only two producing oilfields as late

as 1981. However, more discoveries have been made in the past few years, including a spectacular 1500 BOPD per well producer at Grant Canyon Field.

The exploration difficulties of the vast Great Basin are considerable (Dolly 1979; Foster 1979; Vreeland & Berrong 1979). Within the area are several dozen sub-basins like Railroad Valley, each of which has a unique, sometimes complex sedimentary sequence of heterogeneous alluvial fill, volcanics, metamorphics and sediments. Source rock potential is poorly understood from basin to basin. Most source rocks are immature, but maturity is quite variable due to high heat flow gradients in some areas (Duey 1983; French 1983). Basement can vary unpredictably from volcanics to sediments to intrusives, as was found when drilling offsets to the Grant Canyon discovery. Due to complex deposition and erosion sequences, traps may be found either in structural highs or lows. The traps also occur in a variety of lithologies, including ignimbrites, younger lacustrine shales, and Palaeozoic marine carbonates.

Seismic exploration in this area is particularly challenging (Vreeland & Berrong 1979). Steep dips, complex basement faulting, extensive volcanics, and strong velocity gradients require 24-fold common midpoint data. Soft, saturated surface conditions prohibit the use of heavy vehicles,

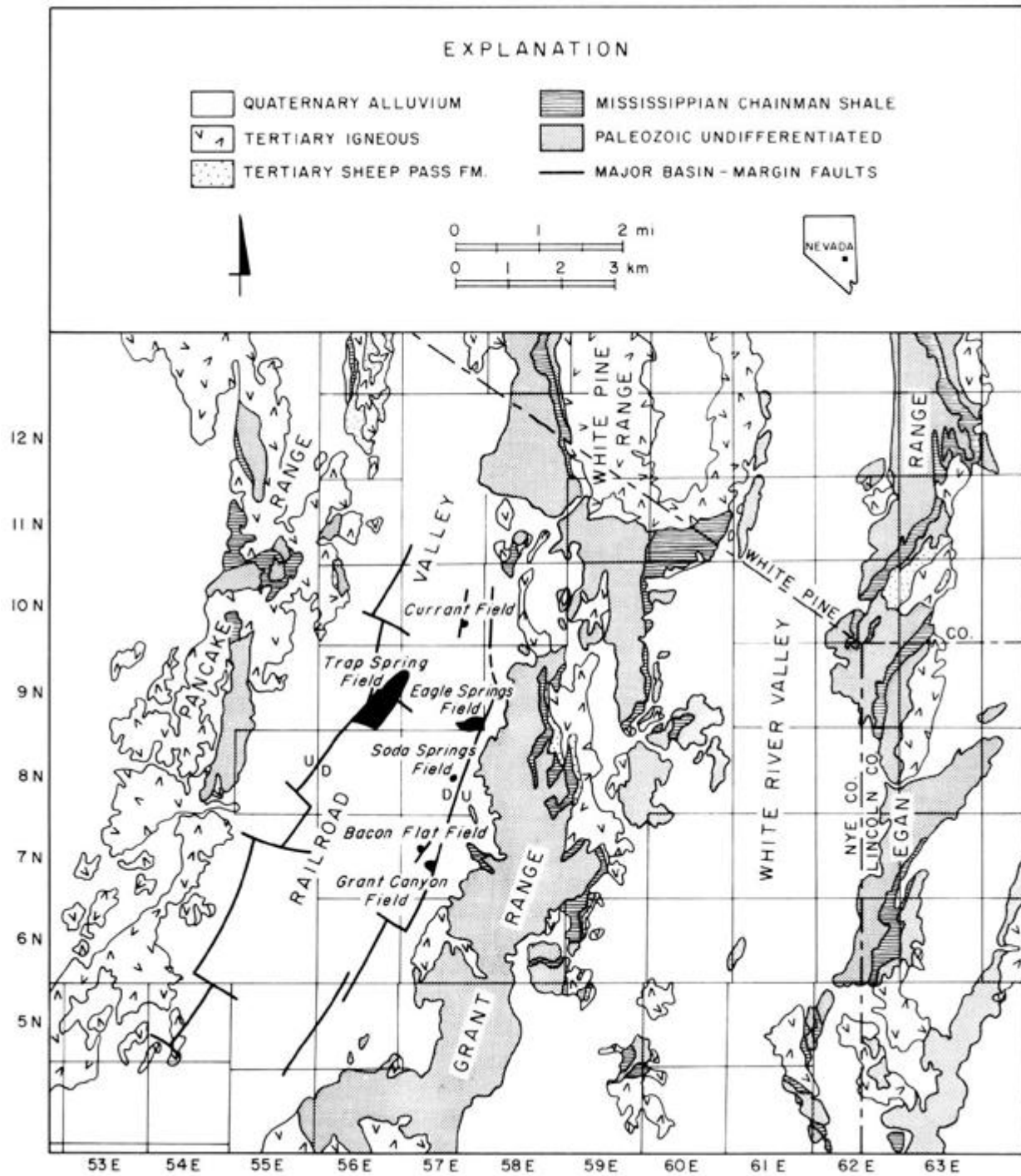


Fig. 4. Generalized geologic map of Railroad and White River Valleys. Railroad Valley fields are found along basin-margin graben faults at the western and eastern boundaries of the valley. Map adapted from French (1983), with additional information from Duey (1983) and recent drilling data.

requiring dynamite surveys for the required bandwidth. In many cases, the resulting data define the structural relationships quite well, as illustrated in the migrated section across Railroad Valley (Fig. 6). However, dynamite data can be of variable quality due to poor signal coupling in dry, heterogeneous bajada slopes at the edges of the basins.

Interpretation problems abound. In some areas volcanic

lenses are found within the alluvial overburden, creating strong multiples which obscure interpretation of the deeper basement materials (Fig. 7). In other areas, gravity-slide masses in the alluvial cover may confuse the interpretation. Nevada's first oilfield, Eagle Springs, was drilled quite fortuitously on a gravity-slide 'high' which is unrelated to the structure at depth. The volcanic/Palaeozoic contact is

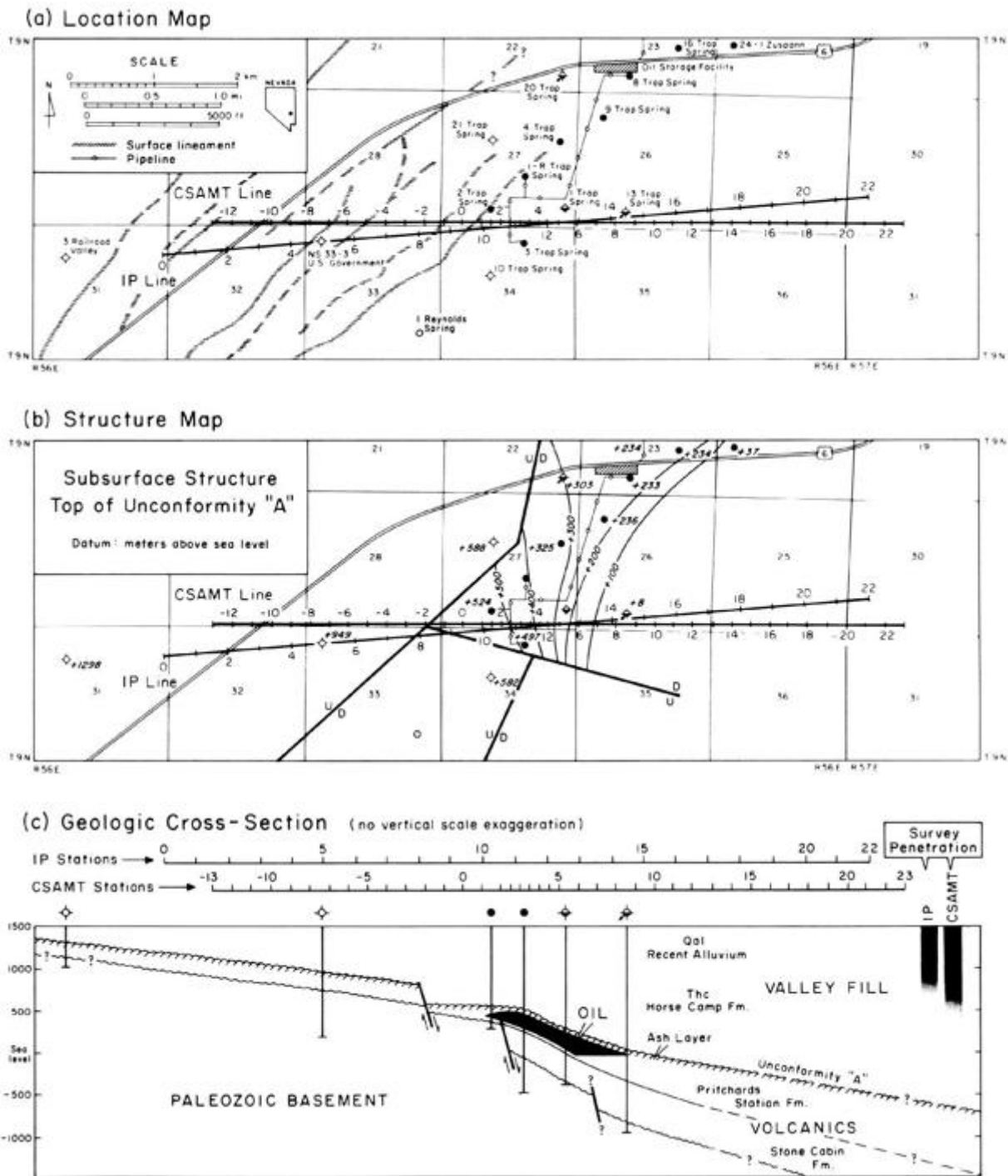


Fig. 5. (a) Location map of electrical survey lines. (b) Structure map, contoured at the top of unconformity 'A', from Duey (1983). (c) Generalized east-west cross-section of Trap Spring Field, adapted from Duey (1978). Side-bars show the maximum depths of penetration of the IP and CSAMT surveys.

sometimes hard to pick because of insufficient velocity contrasts or inhomogeneities in the overburden. Complex faulting patterns are frequently hard to distinguish, especially along basin margins. Finally, the sealing of various bounding faults generally cannot be ascertained prior to drilling.

Hence, while seismic has been helpful in the Great Basin, the numerous problems inherent to the area make seismic a rather expensive and sometimes unpredictable venture. This suggests the use of a less expensive, reconnaissance technique for upgrading prospects prior to detailed seismic coverage.

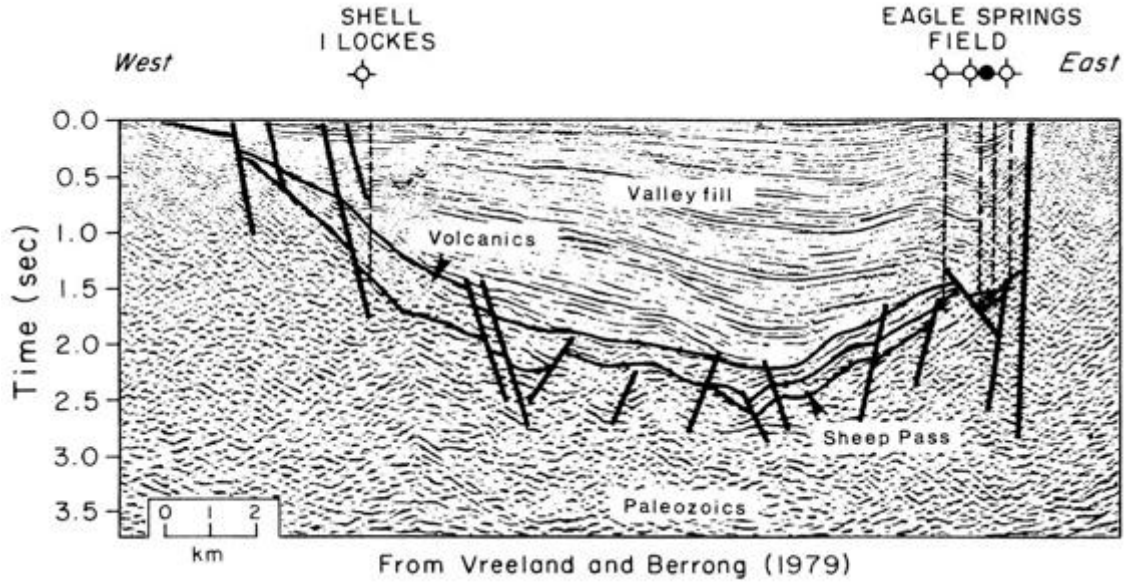


Fig. 6. Typical east-west seismic section across Railroad Valley, from Vreeland & Berrong (1979). The Shell No. 1 Lockes well is located 2.4 km south of No. 2 Trap Spring, which is marked on Fig. 5a.

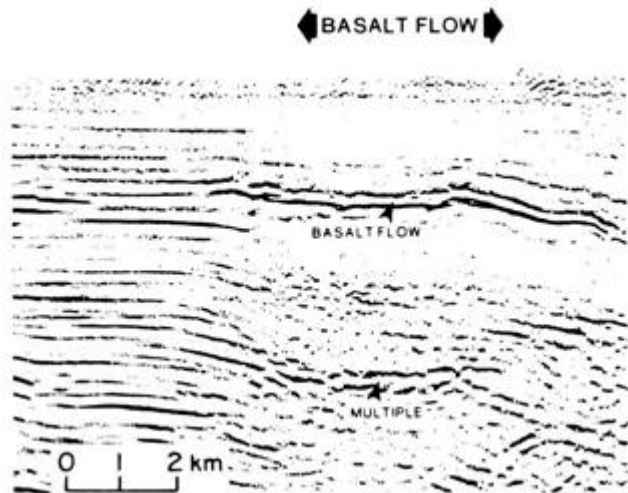


Fig. 7. Seismic section showing the effects of a shallow basalt flow within alluvial fill, from Vreeland & Berrong (1979). The flow is only about 30 m thick, but due to its high velocity (5800 m s^{-1}) it masks deeper features and produces strong multiples. This flow covers large areas of southern Railroad Valley. CSAMT and other electrical techniques will detect such units, but their interpretation is relatively unaffected.

Induced polarization survey

The authors have obtained two different sets of electrical data at Trap Spring Field: induced polarization (IP) and CSAMT. Prior to examining the CSAMT data, it is instructive to outline the results of the IP survey.

Three lines of frequency-domain, dipole-dipole IP data were run over Trap Spring Field using three two-channel, digital receivers (Hughes 1983). The work involved an a-spacing (dipole length) of 381 m and n-spacings (number of dipole lengths between the dipoles) of 1, 2, 3, 4, 5 and 6.

Magnitude and phase data were obtained at frequencies of 0.125, 0.25, 0.5 and 1.0 Hz. Only the data for line 3 of the survey are presented here, since this line was run nearly coincident with the CSAMT line. The maximum depth of penetration of this data set is approximately 800 m.

The apparent resistivity data at 0.125 Hz are presented in Fig. 8a. The data show high-over-low resistivity layering and some lateral character. The broad zone of low resistivities at depth is strongest in the vicinity of the cased wells. Well casings can cause strong conductive and polarization effects in IP data due to current coupling into the steel casings.

The well-casing effect over Trap Spring Field was estimated using the algorithm of Holladay & West (1984), which calculates the DC effects due to infinitely-long, cylindrical casings embedded in an homogeneous half-space. Modelling included all cased wells within three dipole spacings of the line. Input parameters included a 24.5-cm outside pipe diameter, a casing resistivity of 2.0×10^{-7} ohm-m, and an average back ground resistivity of 25 ohm-m. The results for apparent resistivity are shown in Fig. 8b. A strong low-resistivity effect is calculated for the vicinity of the cased wells.

One can remove the calculated well-casing effect from the original data by converting the model results to a percentage of the assumed background resistivity, then dividing the resistivity data by these numbers. The result is the residual apparent resistivity data, shown in Fig. 8c. New, localized and diagonally constrained features appear in the residual data, suggesting that the model has overcorrected somewhat by calculating too large a well-casing effect (overcorrection is noticed on the other two survey lines as well). However, the residual data are useful for an initial evaluation of

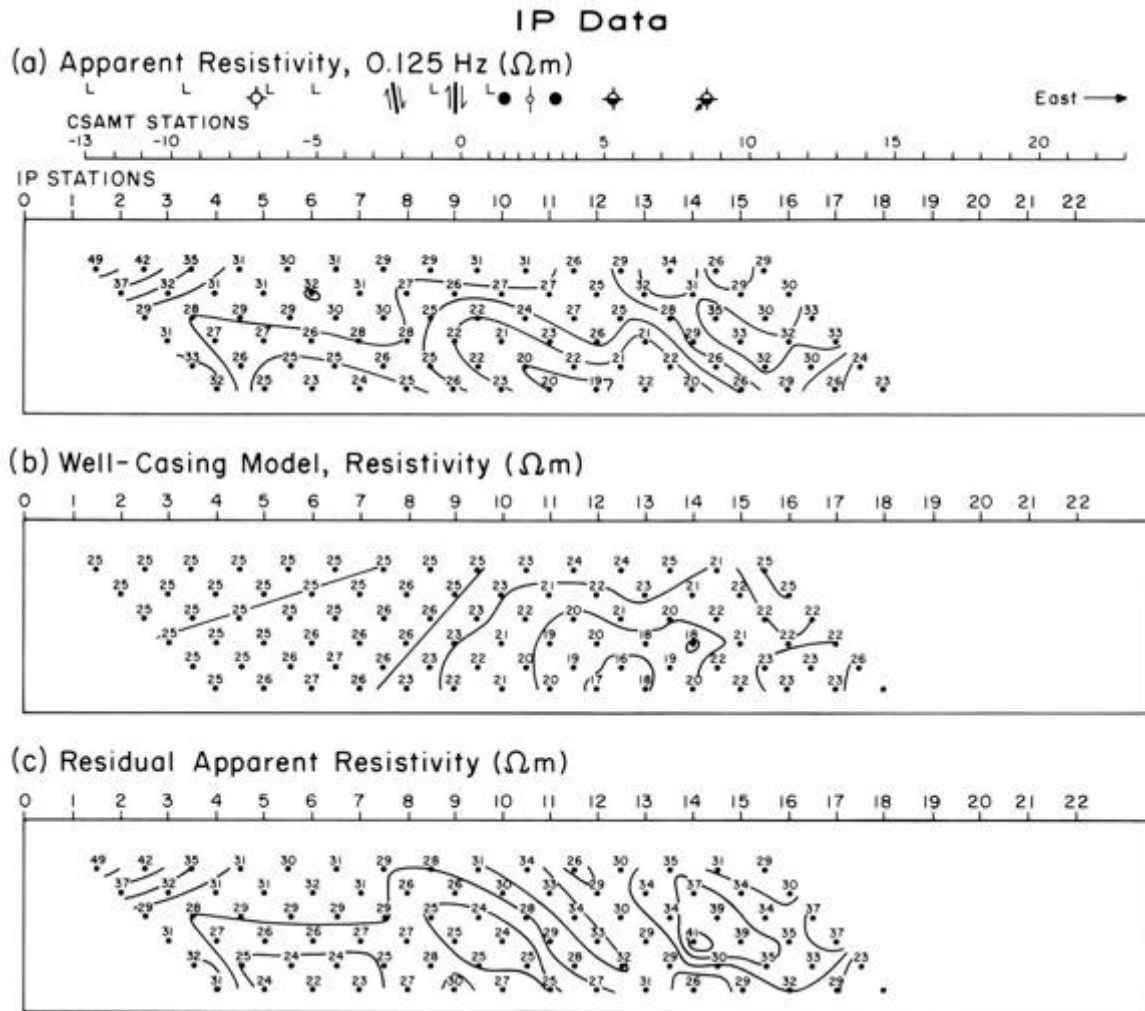


Fig. 8. Apparent-resistivity data and well-casing model results from Line 3 of the IP survey at Trap Spring. See text for details on the well-casing model. The top shows CSAMT and IP station numbers, faults, wells, a surface pipeline (small circle with a vertical bar), and surface lineaments from air photos ('L').

structural effects. The residual data show increasing surface resistivities towards the west, where bajada sediments show less water saturation. The low-resistivity zone at depth may reflect the lower portions of the Horse Camp sediments, which are shown by well logs to be much more conductive than the surface. As expected, this conductive zone deepens towards the east, where the sediments are deeper. Note that the graben fault zone appears to be electrically conductive in the residual data. However, near-surface effects and possibly over-modelling complicate the interpretation by causing diagonal effects.

The phase data are shown in Fig. 9a. As before, a strong effect — this time a polarization high — is found near the cased wells. The algorithm of Holladay & West (1984) was used to calculate the worst-case polarization response, as shown in Fig. 9b. Again, the model may have overcorrected for well-casing effects, but the residual data (Fig. 9c) tend to show structure more clearly. West of the graben fault, the surficial over burden is more polarizable. East of the fault,

the surface is less polarizable than are the deeper sediments. The conductive fault zone also appears to be slightly less polarizable than surrounding sediments. A strong diagonal effect, possibly due to the pipeline at station 10.7, complicates the picture.

The IP data offer interesting results, but the poor resolution and the cultural effects inherent in these types of data argue for a higher-resolution electrical technique such as CSAMT for mapping structure.

CSAMT survey

A controlled source audio-frequency magnetotellurics (CSAMT) survey was run as a follow-up to the IP study (Hughes 1984). A two-channel, digital receiver of the same type used in the IP study was used for the CSAMT work. The survey used a grounded dipole source 2.1 km in length and located 8.1 km north of the survey line. Scalar CSAMT data were obtained, measuring the electric field with a dipole 229 m in length, and the magnetic field with a high-gain

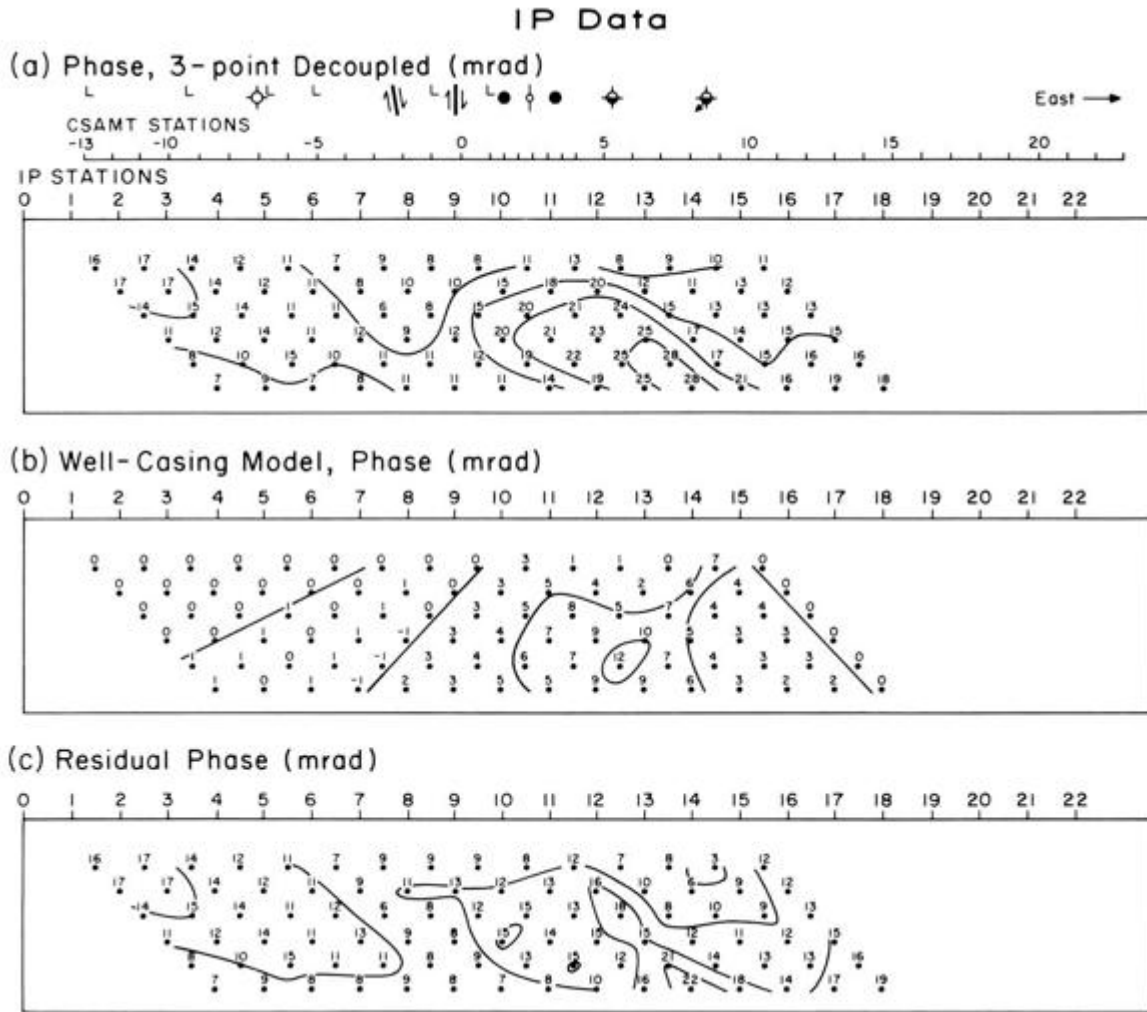


Fig. 9. Phase data and well-casing model results from Line 3 of the IP survey at Trap Spring. Data are calculated for the DC case. See text for details on the well-casing model.

ferrite-core antenna. Both magnitude and phase data were acquired. The frequency range used in the survey was 2 to 4096 Hz, in binary-incremented steps. Given the resistivities encountered in the survey, this fixed the maximum depth of penetration at approximately 1100 m. The survey line location is shown in Fig. 5a.

The CSAMT Cagniard resistivity and phase-difference data are shown in Fig. 10. These data show significantly better resolution and interpretability than the IP data. The vast majority of data have a precision of better than 5%, which corresponds to about ± 1 ohm-m at typical station resistivities of 20 ohm-m. Slightly higher noise levels (up to 10% in some cases) are present in the 4096 and 2048 Hz data at some stations.

The pseudosection of Fig. 10 shows a number of layer-like and lateral features. These can be divided into three types of effects: geometric (near-field and transition zone) effects, static effects, and stratigraphic/structural effects.

Geometric effects are apparent in the horizontal contours

below 16 Hz on the west half of the line. The deep low-resistivity zone is the transition-zone notch, and the steep rise in resistivities below the notch is the beginning of the near-field zone. The transition-zone and near-field behaviour is fairly typical except for one fact — they occur at higher than expected frequencies in this data set. Given an average resistivity of 20 ohm-m and the 8.1-km source/sounding separation, for example, one would calculate that the data would go into the transition zone at about 8 Hz, whereas the transition zone actually begins at 16 Hz. Zonge & Hughes (1988) suggest that this is an artefact of source overprint, wherein the more electrically resistive bajada geology beneath the source affects the transition zone behaviour as measured at the sounding location.

The overprint effect does not seriously inhibit interpretation of this data set. In fact, the overprint-enhanced transition zone is highly sensitive to resistivity layering, and thus enhances the interpretation. The steep notch responds to the strong low-over-high resistivity

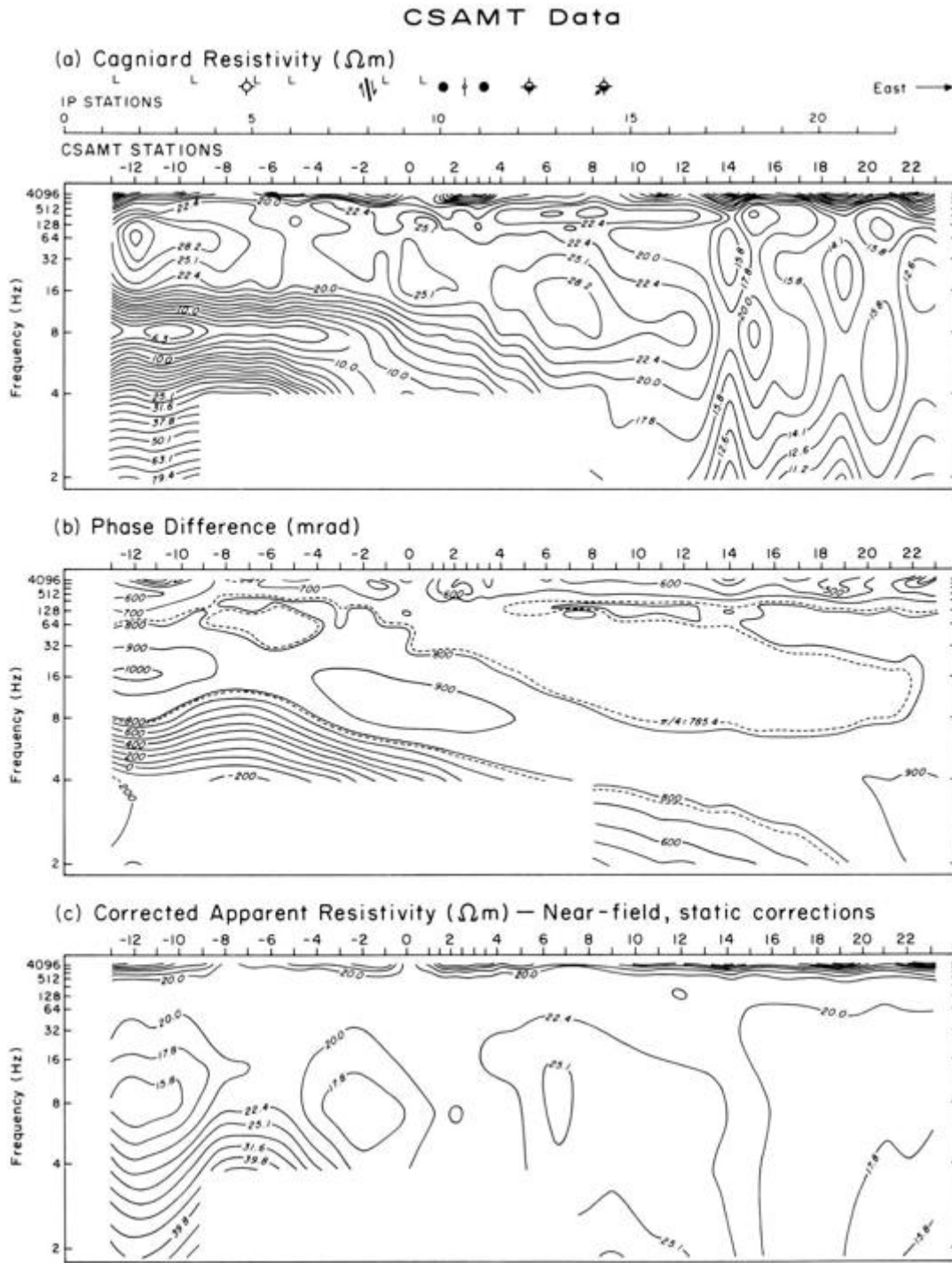


Fig. 10. CSAMT data from Trap Spring Field. (a) Cagniard resistivity data. (b) Phase-difference data. (c) Apparent-resistivity data corrected for static and near-field effects. Data precision is better than $\pm 5\%$ at all but the highest two frequencies.

contrast at the interface between the Horse Camp sediments and the underlying volcanics. Of special interest is the steep drop-off of the notch east of CSAMT station -2. This corresponds almost exactly to the sub surface location of the controlling graben fault. The drop-off shifts the transition zone notch from 8 Hz to approximately 5 Hz. For an

average resistivity of 15 ohm-m, this change in frequency corresponds roughly to a vertical offset of roughly 130 m.

This is approximately the known vertical throw of the fault. The steep easterly dip of the fault is also clearly seen in the data set. The data also suggest additional, smaller faults with down dropped eastern blocks. This again is

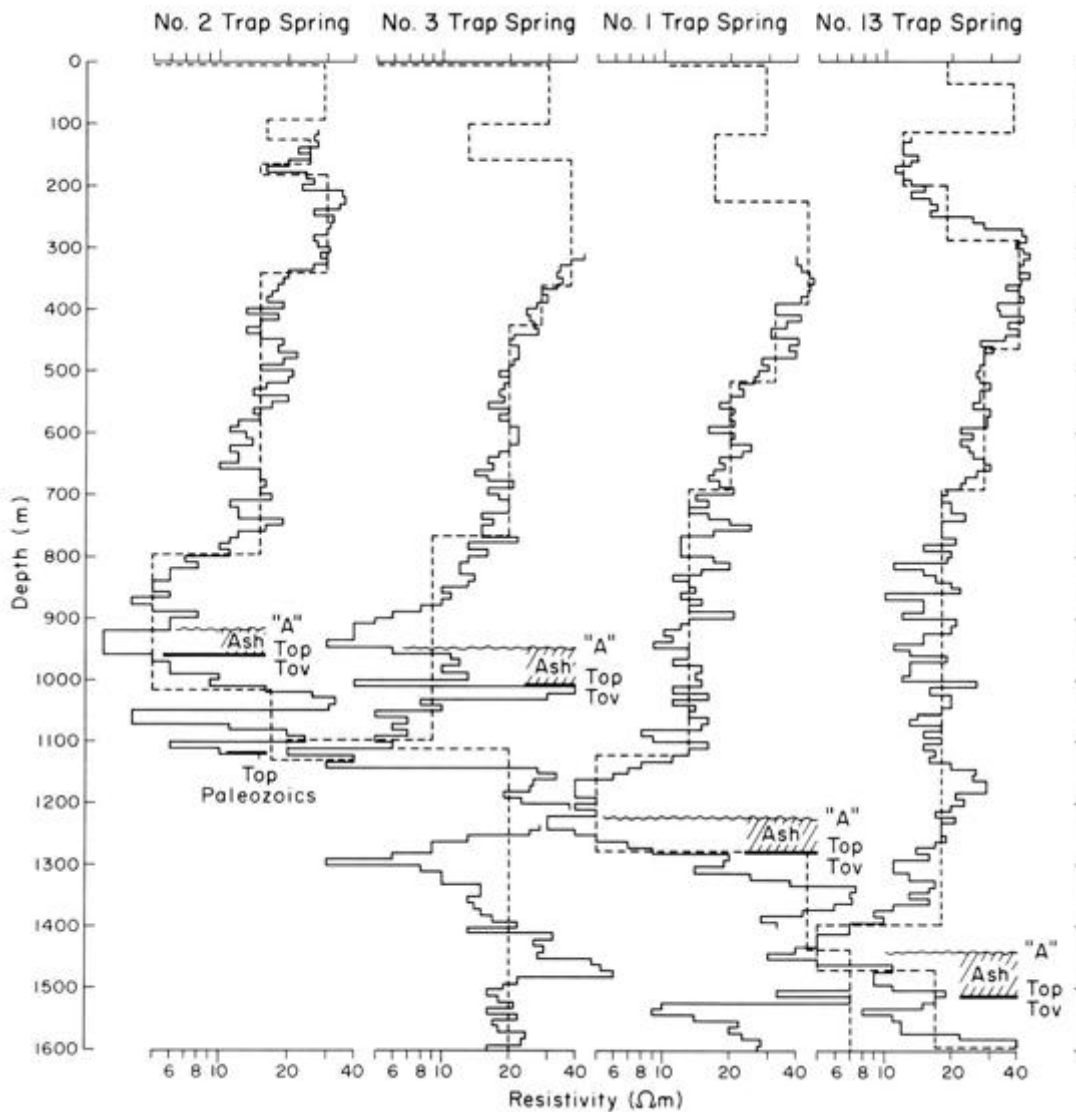


Fig. 11. Digitized deep-induction logs for Trap Spring Field. Dotted lines indicate the simplified layered models used to forward-model the CSAMT data, as described in the text. Note that the logs do not start from the surface, necessitating the insertion of surficial layers required for the modelling.

consistent with known geology (Duey 1979). Finally, the transition zone drops beneath the penetration range of the data on the eastern part of the line, reflecting the deepening of basement towards the centre of Railroad Valley.

The second category of effects evident in the data involves static offset. The effect is best seen by comparing the Cagniard resistivity data (Fig. 10a) to the phase-difference data (Fig. 10b). The resistivity data show an up-and-down appearance from station to station, especially towards the east. Plots of log-resistivity versus log-frequency show that many of these station-to-station changes are frequency-independent shifts characteristic of static effects. The phase data, on the other hand, show a smoothly layered appearance without the laterally variable character of the resistivity data. This occurs because phase is conceptually related to the time

derivative of resistivity, and hence is insensitive to frequency-independent offsets like static offsets.

Since phase data are unaffected by static effects, Zonge & Hughes (1988) have proposed an algorithm for static correction which involves an interpretation of phase data. The integrated data are offset based upon the average resistivity response over a specified set of stations and frequencies. The algorithm was applied to the Trap Spring data. The results, corrected for near-field effects, are shown in the corrected apparent resistivity data of Fig. 10c. Note that many of the laterally variable effects evident along the eastern third of the line in the Cagniard resistivity data are removed in the corrected data. This suggests that these features may be due to localized, surficial changes in alluvial composition and interstitial waters. Such effects were

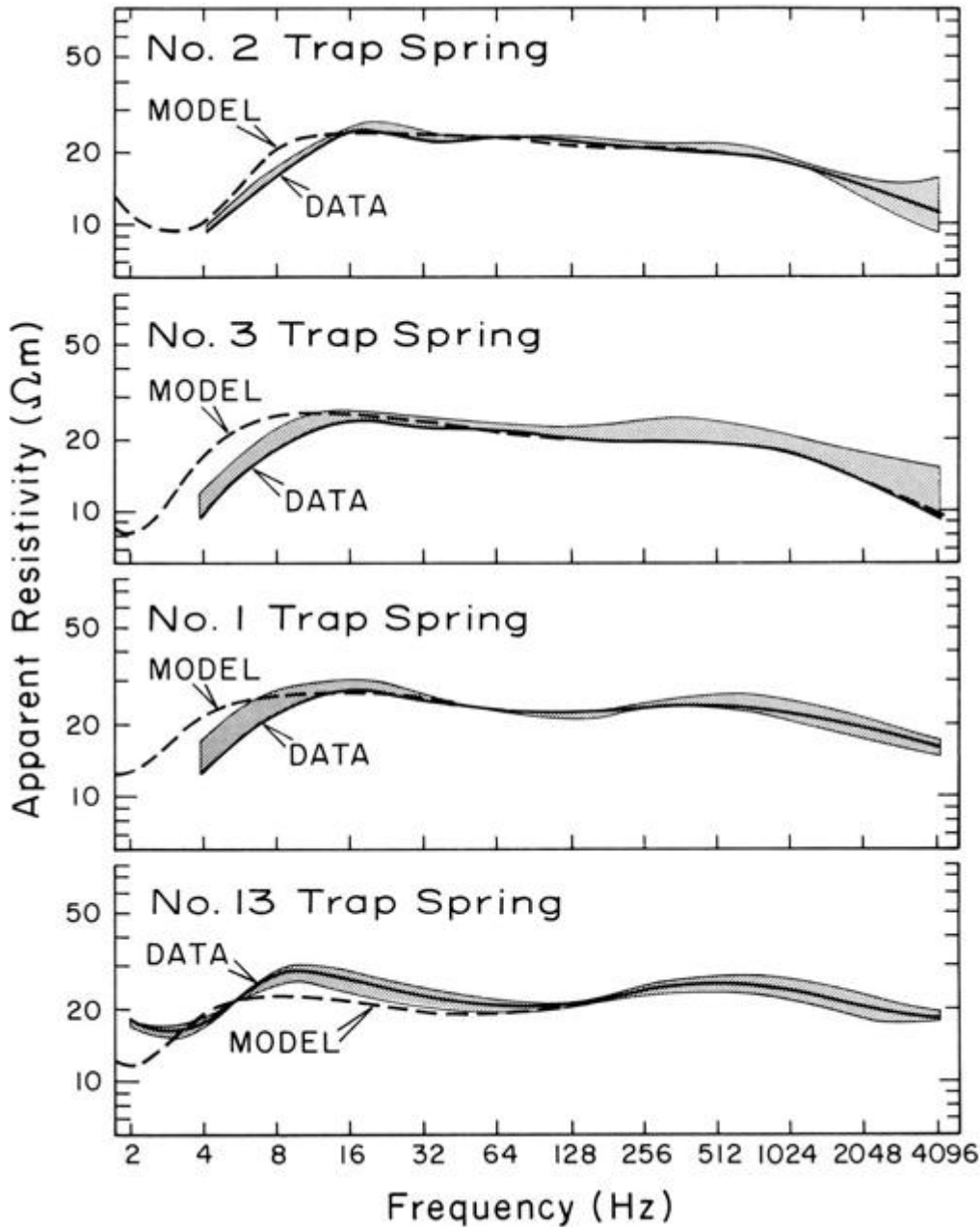


Fig. 12. Comparison of the models generated by the deep-induction log data (dashed lines) and the CSAMT data (solid lines). The shaded area indicates the resistivity range of the several stations in the immediate vicinity of the boreholes.

observed in the IP data, although they affected IP more adversely due to that technique's strong geometric control.

It is useful to note that, unlike the IP data, the CSAMT data appear to be unaffected by cultural contamination from the cased wells or the pipeline. This is an observation typical of many data sets examined by the authors. The relative insensitivity of CSAMT to culture is related to several factors. First, the mechanism of signal coupling is primarily inductive in nature, allowing vertical sounding without significant side-looking effects. This minimizes off-

line culture contamination. In contrast, galvanic IP and resistivity measurements are made in the strongly curved near-field, where culture coupling is maximized and side-looking is significant. Secondly, since CSAMT measurements are made far from the signal source, there is less direct current channelling into cultural features from the source directly to the receiver. Thirdly, the geometric control of IP surveys causes a larger section of the pseudosection to be affected by culture than with CSAMT. For example, a single pipeline could affect a large, pie-

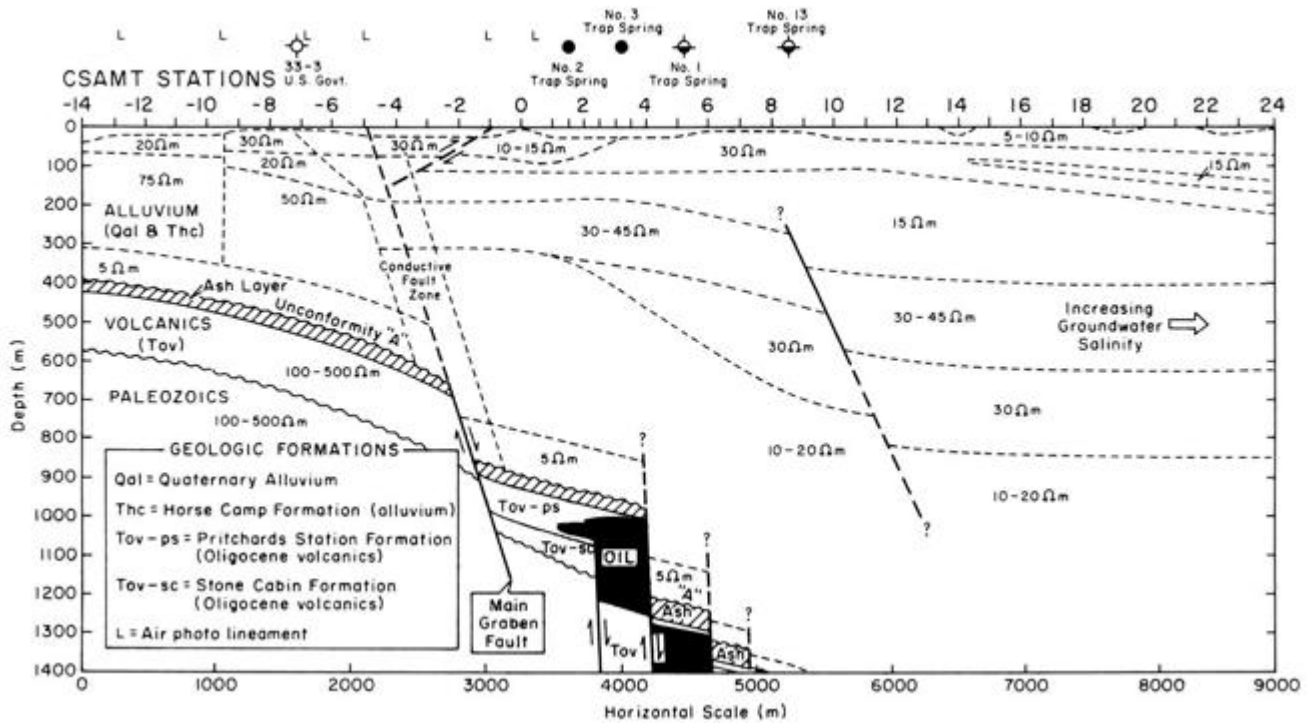


Fig. 13. Interpreted electrical/geologic cross-section of Trap Spring Field, based upon the CSAMT survey and well-log data. The integrated interpretation of the two data sets provides more detail than either data set by itself. Most detail at and above the top of the volcanics would be ascertainable with CSAMT alone, if no well data were available. Vertical scale exaggeration is 3:1.

shaped section of data in dipole-dipole IP, while the same pipeline would at worst affect only one or two vertical CSAMT soundings.

The third group of effects present in the data is the group we are most interested in — the effects of structure and lithology. The deeper faulting was pointed out in the discussion of geometric effects. However, several other faults are evident in the far-field data. Of particular interest is the conductive zone which extends from the vicinity of the graben fault and projects to the surface near station -5. This conductive zone may represent a surficial extension of the graben fault system. The static-corrected data suggest that the majority of the conductive response is concentrated towards the surface. The surficial conductor corresponds to the location of a surface lineament (Fig. 5a) identified in infrared air photos (Hughes 1984; Foster 1979).

The fact that the graben fault is conductive suggests that it may be unsealed, at least in respect of brine movement. Other lineaments noted on the air photos do not appear to be conductive, suggesting that they may be sealed faults or may simply be beach ridges or other non-structural features. If this conclusion is correct, it suggests a possible means of determining fault sealing in this environment. However, much more work would be necessary before concluding that CSAMT is adapted to this purpose.

The Cagniard resistivity data show a definite regional trend towards lower resistivities to the east. This trend is correlated with higher groundwater salinity towards the

centre of Railroad Valley (Van Denburgh & Rush 1974; Duey 1983). The surficial low resistivities reflect the fact that surface waters are more saline than deeper waters in this area, the reverse of the normal trend.

Lithology is well shown in the CSAMT data. Besides the strong alluvium / basement contact, one also can see a number of layers within the alluvium itself. These layers correspond quite well to layers seen in resistivity logs. The lower layer above the volcanics is quite conductive due to its high clay content. The clay-rich, heavily altered ash zone at the very top of the volcanics is the most conductive, and this contributes to the strong conductive gradient at the lower frequencies of the CSAMT data.

A direct comparison between well logs and the CSAMT data was made to illustrate the resolving ability of surface CSAMT surveys. Dual induction logs from the four wells along the CSAMT line were digitized and the logarithm of resistivity plotted versus depth, as shown in Fig. 11 (no dual induction well log was available for the No. 33-3 US Government well). The digitized logs for each well were then subdivided into representative resistivity layers, and these were used for forward modelling of the CSAMT responses. Since the logs do not go all the way to the surface, several surface layers were added to the models; resistivities and thicknesses of these surface layers were varied iteratively in order to obtain a best fit to the CSAMT data. Fig. 12 shows the comparison of the models (dashed lines) to the CSAMT resistivity response (solid lines) for

stations in the immediate vicinity of the modelled well logs.

The results show a good to excellent correlation between logs and the surface geophysics in the four wells modelled. The transition-zone match is poor at all four wells because of the source overprint noted earlier. However, the far-field correlation is quite good. Hence, while CSAMT lacks the fine resolution of the logging tool, it nevertheless is useful in mapping major changes in layering without relying upon drilling wells for data acquisition.

Based upon the previous discussion, the final interpreted section of Fig. 13 was prepared. This interpretation is based upon all the CSAMT, IP, and geologic information available to the authors; however, the picture would not change substantially in the more usual event that geologic information was not available. The amount of detail provided by the interpretation, while not approaching that of the seismic section of Fig. 6 is still quite sufficient for locating the main structural features over Trap Spring Field and showing the major lithologic and structural relationships of interest.

Conclusions

The Trap Spring data demonstrate the ability of CSAMT to map major structure and stratigraphy in frontier basin environments. The CSAMT data are clearly superior to dipole-dipole IP in this application. Although CSAMT lacks the resolution inherent to seismic data, it is fully capable of mapping the more significant structural features seen in seismic sections at depths of about 2 km or less. Its resolution of stratigraphy may actually be better than seismic in certain areas where the alluvium / volcanic interface is hard to pick in seismic data. In addition, the presence of volcanic lenses or gravity slides within valley fill would produce much less of an effect on interpretation of the CSAMT data than they would with reflection seismics. Finally, CSAMT may be run at approximately one-sixth the cost of 24-fold CMP dynamite surveys for the same length of profile.

Thus, CSAMT shows considerable promise in mapping sub-basins like Railroad Valley on a reconnaissance basis. The CSAMT work then could be used to qualify prospects worthy of final detailing with seismic. The proper combination of electrical and seismic could reduce by a considerable amount the overall geophysical expenditures required to locate and upgrade a drilling prospect. This kind of an integrated, multi-phase exploration strategy could be applicable to a number of frontier areas world-wide.

In addition to its reconnaissance function, CSAMT offers three additional uses in the context of an existing seismic exploration programme. First, CSAMT can be useful in locating potential problem areas for seismic in advance of the seismic survey. Such problem areas, for example, might include high-velocity gradients associated with volcanic layers or coal seams or local zones of severe surface weathering. Second, CSAMT data can be used to help process and interpret seismic data when additional control

on near-surface geology is needed. Third, in areas where seismic is limited, such as basalt-covered terrains and complex overthrust environments, CSAMT can be used as a primary exploration tool.

The integrated use of seismic, electrical techniques such as CSAMT, and other methods could help reinvigorate the exploration effort in many of the world's more difficult exploration environments.

Acknowledgments

The authors would like to thank Zonge Engineering for its financial support of the field work, the Rocky Mountain Association of Geologists for permission to reproduce the seismic data, and Herb Duey for helpful information on Railroad Valley geology. We would also like to thank Anne Urizar for her excellent drafting.

Received 23 December 1986; accepted 8 July 1987.

References

- ANDRIEUX, P. & WIGHTMAN, W.E.D. 1984. The so-called static corrections in magnetotelluric measurements. 54th SEG Meeting, Atlanta, USA, Expanded Abstracts, 43-44.
- BARTEL, L.C. Potential use of the CSAMT geophysical technique to map UCG processes. In: Proceedings of the 8th underground coal conversion symposium, 59-57.
- BARTEL, L.C. & DOBECKI, T.L. 1982. Geophysical applications in coal exploration and mine planning: electromagnetics. Proceedings of the SME-AIME Annual Meeting, Dallas, Texas. SME Reprint 82-97, 1-9.
- BARTEL, L.C. & JACOBSON, R.D. 1987. Results of a CSAMT survey at the Puhimau Thermal area, Kilauea Volcano, Hawaii. Geophysics 52, 665-667.
- BARTEL, L.C. & WAYLAND, J.R. 1981. Results from using the CSAMT geophysical technique to map oil recovery processes. 56th Fall Conference of the Society of Petroleum Engineers of AIME, San Antonio, Texas. SPE Reprint 10230, 1-9.
- DOLLY, E.D. 1979. Geological techniques utilized in Trap Spring Field discovery, Railroad Valley, Nye County, Nevada. In: Basin and Range Symposium, G.W. Newman & H.D. Goode (eds), Rocky Mountain Association of Geologists and Utah Geological Association, 455-467.
- DUEY, H.D. 1978. Trap Spring. In: Oil and Gas Fields of the Four Corners Area, J.E. FASSET (ed), Four Corners Geological Society, 1, 174-175.
- DUEY, H.D. 1979. Trap Spring Oilfield, Nye County, Nevada. In: Basin and Range Symposium, G.W. Newman & H.D. Goode (eds), Rocky Mountain Association of Geologists and Utah Geological Association, 469-476.
- DUEY, H.D. 1983. Oil generation and entrapment in Railroad Valley, Nye County, Nevada. Geothermal Resources Council, Special Report No. 13, 199-205.
- FOSTER, N.H. 1979. Geomorphic exploration used in the discovery of Trap Spring Oilfield, Nye County, Nevada. In: Basin and Range Symposium, G.W. Newman & H.D. Goode (eds), Rocky Mountain Association of Geologists and Utah Geological Association, 477-486.
- FRENCH, D.E. 1983. Origins of Oil in Railroad Valley, Nye County, Nevada. American Association of Petroleum Geologists Bulletin 67, 1337 (abstract).
- FRENCH, D.E. & FREEMAN, K.J. 1979. Tertiary volcanic stratigraphy and reservoir characteristics of Trap Spring Field, Nye County, Nevada. In: Basin and Range Symposium, G.W. Newman & H.D. Goode (eds), Rocky Mountain Association of Geologists and Utah Geological Association, 487-502.

- FRYBERGER, J.S. & TINLIN, R.M. 1984. Pollution potential from injection wells via abandoned wells. Proceedings of the 1st National Conference on Abandoned Wells: Problems and Solutions. Environmental and Ground Water Institute, University of Oklahoma, 84-117.
- GOLDSTEIN, M.A. & STRANGWAY, D.W. 1975. Audio-frequency magnetotellurics with a grounded electric dipole source. *Geophysics* 40, 669-683.
- HJELT, S.E., HEIKKA, J.V., LAKANEN, M.E., PELKONEN, R. & PIETILA, R. 1987. The audiomagnetotelluric (AMT) method and its use in ore prospecting and structural research. In: Electrical prospecting for ore deposits in the Baltic Shield, issue 2, electromagnetic methods prospecting and structural research, S.E. Hjelt & A.F. Fokin (eds), in press.
- HOLLADAY, J.S. & WEST, G.F. 1984. Effects of well casings on surface electrical surveys. *Geophysics* 49, 177-188.
- HUGHES, L.J. 1983. Case histories of an electromagnetic method for petroleum exploration. Zonge Engineering & Research Organization, Inc., Tucson, Arizona.
- HUGHES, L.J. 1984. Final report on CSAMT survey at Trap Spring Field, Nye County, Nevada: an evaluation of CSAMT for Great Basin petroleum exploration. Zonge Engineering & Research Organization, Inc., Tucson, Arizona.
- HUGHES, L.J., CARLSON, N.R. & OSTRANDER, A.G. 1984. Applications of CSAMT in mapping structure and alteration associated with petroleum. 54th SEG Meeting, Atlanta, USA, Expanded Abstracts, 102-104.
- LAKANEN, E. 1986. Scalar audiomagnetotellurics applied to base-metal exploration in Finland. *Geophysics* 51, 1628-1646.
- LARSEN, J.C. 1981. A new technique for layered earth magneto-telluric inversion. *Geophysics* 46, 1247-1257.
- MONTGOMERY, G.E. 1985. Geophysical activity in 1984. *Leading Edge* 4, 33-54.
- OSTRANDER, A.G., CARLSON, N.R. & ZONGE, K.L. 1983. Further evidence of electrical anomalies over hydrocarbon accumulations using CSAMT. 53rd SEG Meeting, Dallas, USA, Expanded Abstracts, 60-63.
- SANDBERG, S.K. & HOHMANN, G.W. 1982. Controlled-source audiomagnetotellurics in geothermal exploration. *Geophysics* 47, 100-116.
- STERNBERG, B.K., WASHBURNE, J.C. & ANDERSON, R.G. 1985. Investigation of MT static shift correction methods. 55th SEG Meeting, Washington DC, USA, Expanded Abstracts, 264-267.
- STERNBERG, B.K., BULLER, P.L., KISABETH, J.L. & MEHRENTAEB, E. 1984. Electrical Methods for Hydrocarbon Exploration II, Magnetotelluric (MT) Method. In: Unconventional Methods in Exploration for Petroleum and Natural Gas III, M.J. Davidson & B.M. Gottlieb (eds), Southern Methodist University Press, 202-230.
- VAN DENBURGH, A.S. & RUSH, F.E. 1974. Water-resource appraisal of Railroad and Penoyer valleys, east-central Nevada, Water Resources Reconnaissance Series Report No. 60, Nevada Department of Conservation and Natural Resources, Division of Water Resources.
- VREELAND, J.H. & BERRONG, B.H. 1979. Seismic exploration in Railroad Valley, Nevada. In: Basin and Range Symposium, G.W. Newman & H.D. Goode (eds), Rocky Mountain Association of Geologists and Utah Geological Association, 557-569.
- WARNER, B.N., BLOOMQUIST, M.G. & GRIFFITH, P.G. 1983. Magnetotelluric interpretations based upon new processing and display techniques. 53rd SEG Meeting, Dallas, USA, Expanded Abstracts, 151-154.
- WAYLAND, J.R. JR & LEIGHTON, A.J. 1985. Mapping technology: a key to EOR control. *Oil and Gas Journal*, 109-115.
- WAYLAND, J.R. JR, LEE, D.O. & CABE, T.J. 1984. Mapping of a streamflood in a Utah tar sand by controlled source audio magnetotelluric survey. Society of Petroleum Engineers / Department of Energy 4th Symposium on Enhanced Oil Recovery, Tulsa, Oklahoma, 441-446.
- YAMASHITA, M., HALLOF, P.G. & PELTON, W.H. 1985. CSAMT case histories with a multi-channel CSAMT system and near-field data correction. 55th SEG Meeting, Washington DC, USA, Expanded Abstracts, 276-278.
- ZONGE, K.L. & HUGHES, L.J. 1988. Controlled source audio-frequency magnetotellurics. In: Electromagnetic methods - theory and practice, M.N. Nabighian (ed.) Society of Exploration Geophysicists.
- ZONGE, K.L., OSTRANDER, A.G. & EMER, D.F. 1980. Controlled source audio-frequency magnetotellurics measurements. Presented at 50th SEG Meeting, USA, Technical papers 2491-2521.
- ZONGE, K.L., FIGGINS, S.J. & HUGHES, L.J. 1985. Use of electrical geophysics to detect sources of groundwater contamination. 55th SEG Meeting, Washington DC, USA, Expanded Abstracts, 147-149.